

River Discharge Simulation Using Variable Parameter McCarthy–Muskingum and Wavelet- Support Vector Machine Methods

Basant Yadav^{*1}, Shashi Mathur²

¹Cranfield Water Science Institute, Cranfield University,
Cranfield MK43 0AL, UK

²Department of Civil Engineering, Indian Institute of Technology Delhi, India

^{1*}Corresponding author email- basant.yadav@cranfield.ac.uk ; basant1488@gmail.com

ABSTRACT

In this study an extended version of variable parameter McCarthy–Muskingum (VPMM) method originally proposed by Perumal and Price (2013) was compared with the widely used data based model namely support vector machine (SVM) and hybrid wavelet-support vector machine (WA-SVM) to simulate the hourly discharge in Neckar River wherein significant lateral flow contribution by intermediate catchment rainfall prevails during flood wave movement. The discharge data from the year 1999 to 2002 has been used in this study. The extended VPMM method has been used to simulate nine flood events of the year 2002 and later the results were compared with SVM and WA-SVM models. The analysis of statistical and graphical results suggest that the extended VPMM method was able to predict the flood wave movement better than the SVM and WA-SVM models. A model complexity analysis was also conducted which suggest that the two parameter based extended VPMM method has less complexity than the three parameters based SVM and WA-SVM model. Further, the model selection criteria also gives the highest values for VPMM in 7 out of 9 flood events. The simulation of flood events suggested that both the approaches were able to capture the underlying physics and reproduced the target value close to the observed hydrograph. However, the VPMM models is slightly more efficient and accurate, than the SVM and WA-SVM model which are based only on the antecedent discharge data. The study captures the

current trend in the flood forecasting studies and showed the importance of both the approaches (Physical and data based modeling). The analysis of the study suggested that these approaches complements each other and can be used in accurate yet less computational intensive flood forecasting.

Keywords- Flood forecasting, VPMM, SVM, Wavelet Transform

1. Introduction

Accurate forecasting of discharge is extremely important in flood management, reservoir management and hydropower design. The accuracy in forecasting discharge depends on the type of simulation model adopted and a review of literature shows that long term and short term discharge forecasting models are being used extensively in various water management problems such as flood control, drought management, water supply utilities operations, irrigation supply management and sustainable development of water resources. In the last few decades, researchers have proposed many models to improve the accuracy of discharge forecasting. These models can be broadly classified as physically based, conceptual and data driven models. A physically based model include as much of small-scale physics and natural heterogeneity as is computationally possible by considering variables such as groundwater, precipitation, evapotranspiration, initial soil moisture content and temperature (Loague and Vander Kwaak, 2004). These can be further classified as hydraulic and hydrologic routing methods. The hydrologic routing methods are widely used in the field practices since early thirties and they have been developed essentially to overcome the tedious computations involved in the hydraulic routing methods (Perumal et al., 2017). Among the many lumped hydrological routing methods, the Muskingum method introduced by McCarthy (1938) is well known in the literature (Chow et al., 1988). The Muskingum method was studied by Ponce and Yevjevich (1978) resulting in the development of Variable Parameter Muskingum-

Cunge (VPMC) method. However, the VPMC method was criticised for the mass conservation problem (Perumal and Sahoo, 2008). To overcome this problem, Todini (2007) revisited the original Muskingum-Cunge (MC) flood routing approach and suggested that the error in mass conservation occurs due to the use of time variant parameters. Later, Price (2009) proposed a nonlinear Muskingum method as an approximation of the one-dimensional Saint-Venant equations and suggested a way out to include any uniformly distributed time-dependent lateral inflow along the river. Recently Perumal and Price (2013) proposed a fully mass conservative approach to study the flood wave propagation in channels (without lateral flow) named variable parameter Muskingum method based on the Saint-Venant equations. Although, these methods successfully captured the flood wave movements and also tackled the problem of mass conservation, the consideration of lateral flow along the river reach still was the cause for erroneous river discharge prediction. A separate approach was suggested by O'Donnell (1985) to include lateral flow in the Muskingum method assuming that the lateral flow has the same form as the inflow hydrograph as pointed out by Perumal et al. (2001). This concept was further studied by Karahan et al., (2014) using the approach of O'Donnell (1985) to incorporate lateral flow and proposed a nonlinear Muskingum flood routing model. This three parameter based semi-empirical Muskingum method has limitation about its applicability to only those events which were similar to the observed past events. To overcome this problem, Yadav et al., (2015) proposed an extended VPMM method considering uniformly distributed lateral flow along the river reach. This study extended the approach of Perumal and Price (2013) and successfully captured the significant amount of lateral flow due to intervening catchment rainfall. Recently, Swain and Sahoo (2015) also studied the fully mass conservative VPMM model and extended it to exclusively incorporate the spatially and temporally distributed non-uniform lateral flow while routing the flood events for compound river channel flows.

Although a physical method provide reasonable accuracy, their implementation and calibration typically present various difficulties (Nayak et. al., 2007). Moreover, in situations particularly in developing countries where the data about the processes to be modelled is limited, physically based model cannot be built, or they are inadequate. A well-calibrated conceptual model can also provide reasonable simulation accuracy, however, their uses are limited, because entire physical process in the hydrologic cycle is mathematically formulated in the conceptual models. Thus, they are composed of a large number of parameters making the model very complicated and slow. This in turn leads to problems of over parameterization (Beven, 2006) which may manifest itself in large prediction uncertainty (Uhlenbrook et al., 1999). In the last few decades, data driven techniques capable of handling large data sets have been adopted while dealing with water resources problems. In forecasting of river discharge, data-based hydrological methods are gaining popularity because they can be developed very rapidly with requirement of minimal information (Yadav et al., 2016b). Though they may lack the ability to provide a physical interpretation and insight into the catchment processes, they are nevertheless able to forecast relatively accurate discharge values (Adamowski and Sun, 2010). The lack of extensive data and cost of collection coupled with inaccessibility of sites compels one to select models based on past recorded flow data while simulating river flow variability (Kisi, 2008, Shiri and Kisi, 2010). Further, data-driven models that operate on an interrelationship between input-output data only without capturing the complete dynamics of the system, may therefore be preferred in certain cases (e.g., in contexts of limited data).

With the advent of computers and the availability of high computational facilities, many researchers have employed data driven techniques while forecasting discharge (e.g., Dawson and Wilby 1998; Sudheer et al. 2002; Shiri et al., 2012; Ghalkhani et al., 2013; Badrzadeh et al., 2013; Rezaeianzadeh et al., 2014; Kasiviswanathan et al, 2016). Much

research has been carried out in the recent past on the use of artificial neural networks (ANN) for discharge forecasting since it is reliable and promising and plethora of literature is available with its applications. Study of hydrological processes using data based models mainly depends on the time series of the considered process. The length of the time series is also important as it captures the short term and long term trend of the process, which can also help in accurate simulation and prediction of the future events. The neural network based models were also used successfully for the trend analysis of time series (Maier and Dandy, 2000; Rafael et al., 2011; Lin et al., 2017). Similarly, Genetic programming (Koza, 1992) is another data based approach which has been successfully applied to many studies in water resources engineering problems. However, the most notable one was the support vector machine (SVM), a kernel based technique based on the Vapnik–Chervonenkis (VC) theory (Vapnik, 1995). The main advantage of this relatively new machine learning method is that it not only possesses the strengths of ANN but is able to overcome the problems associated with local minimum and network over fitting (ASCE Task Committee on Application of Artificial Neural Networks in Hydrology, 2000). Further, despite the flexibility and usefulness of data driven methods in modeling hydrological processes, they have some drawbacks with highly non-stationary responses or seasonality (Cannas et al., 2006, Tiwari and Chatterjee, 2010, Adamowski and Chan, 2011, Nourani et al., 2014). To handle such problems a method called wavelet analysis (WA) has been used in various hydrological studies. Sang (2013a) highlighted that the understanding of hydrologic series can be improved from wavelet analysis. Recent application of wavelet analysis in hydrological modeling (Kalteh, 2013, Suryanarayana et al., 2014, Agarwal et al., 2016, Yadav et al., 2017) suggest that the WA approach provides a superior alternative to the data driven models and can enhance the accuracy by developing the more detailed input–output combinations. In light of the above facts, an attempt has been made herein to assess the abilities of the wavelet

127 based support vector machine to predict the discharge in a river reach where the lateral flow
128 is very significant. Further, we also intend to compare the two distinctively discharge
129 prediction approaches to suggest an accurate yet less complex discharge prediction method
130 for such a catchment conditions. The techniques were experimented on a 24.2 km stretch of
131 Neckar River between Rottweil and Oberndorf.

132 **2. Methodology**

133 **2.1 Variable parameter McCarthy–Muskingum (VPMM)**

134 The fully mass conservative VPMM was developed by Perumal and Price (2013). After a
135 decade of research, VPMM is capable to conserve volume absolutely and also follow the
136 heuristic assumption of the prism and wedge storage established by McCarthy (1938) in the
137 development of the classical Muskingum method. The method fundamentally makes use of a
138 parallel approach followed by Perumal (1994a, 1994b) in the development of the VPM
139 routing method. The VPMM method is developed from an approximation of the momentum
140 equation of the Saint-Venant equations. This approximation is applied directly to the one-
141 dimensional continuity equation of the Saint-Venant equations, leading to a fully
142 conservative routing method which has the same routing equation as the classical Muskingum
143 method proposed by McCarthy in (1938). The use of hydraulic principle in the development
144 of the VPMM method allow the characterization of the considered channel reach storage into
145 prism and wedge storage which complies with the heuristic assumption of McCarthy (1938)
146 who developed the Muskingum method. The equation derived in the VPMM method for the
147 travel time and weighting parameter is same as the classical Muskingum method and based
148 on the flow and channel characteristics. The equations governing the one-dimensional
149 unsteady flow in channels and rivers are given below (Perumal and Price (2013) as

150

151
$$\frac{\partial Q}{\partial x} + \frac{\partial A}{\partial t} = 0 \quad (1)$$

152
$$S_f = S_o - \frac{\partial y}{\partial x} - \frac{v}{g} \frac{\partial v}{\partial x} - \frac{1}{g} \frac{\partial y}{\partial t} \quad (2)$$

153 The Eq. (1) and (2) represents the continuity and momentum equation, respectively. The
 154 discharge at any section of the routing reach using the VPMM method can be obtained using
 155 the equation as (Perumal and Price (2013) as

156
$$Q_M = Q_{o,M} \left\{ 1 - \frac{1}{S_o} \frac{\partial y}{\partial x} \left[1 - \frac{4}{9} F_M^2 \left(\frac{P}{B} \frac{dR}{dy} \right)_M^2 \right] \right\}^{1/2} \quad (3)$$

157 where, t is the time; x is the distance along the channel; y is the flow depth; v is the average
 158 cross-sectional velocity; A is the cross-sectional area; Q represents the discharge; g is the
 159 acceleration due to gravity; S_f is the frictional slope; S_o is the bed slope; $(\partial y / \partial x)$ is the
 160 longitudinal gradient of water profile; $(v/g)(\partial v / \partial x)$ is the convective acceleration slope and
 161 $(1/g)(\partial v / \partial t)$ is the local acceleration slope; P_M , B_M and R_M , respectively, represents the
 162 wetted perimeter, top width and hydraulic radius corresponding to flow depth y_m . The
 163 notation Q_M is the average discharge at the mid-section of the reach at any time and $Q_{o,M}$ is
 164 the normal discharge at the midsection corresponding to flow depth y_m and F_M is the Froude
 165 number.

166 The developed VPMM method was further modified to account lateral flow in flood
 167 routing study using the similar approach suggested by O'Donnell (1985). Though, the
 168 fundamental principle remains same, lateral flow was incorporated in a distributed form
 169 throughout the river stretch (Fig. 1). For the detailed explanation on the lateral flow
 170 estimation approach readers can refer to Yadav et al., (2015). Accordingly, the lateral flow

171 hydrograph q_L is assumed to have the similar shape as the inflow hydrograph and it is
 172 supplied uniformly along the river stretch at each time interval. Hence, the original continuity
 173 equation in the VPMM method is modified as

$$174 \quad \frac{\partial Q}{\partial x} + \frac{\partial A}{\partial t} = q_L \quad (4)$$

175 where, q_L is the lateral flow per unit length of the channel.

176 The contribution of lateral flow in the river stretch is assumed to be perpendicular to the
 177 channel reach, hence the channel flow receives no or very negligible momentum.
 178 Accordingly, in the modified VPMM method the momentum equation (Eq. (2)) remains
 179 unaltered. The modified continuity equation and the original momentum equation were
 180 further solved to account the uniformly distributed lateral flow and the approach arrived at
 181 following (Yadav et al., 2015) as

$$182 \quad Q_{i+1}^{j+1} = C_1 Q_i^{j+1} + C_2 Q_i^j + C_3 Q_{i+1}^j + C_4 q_{Lavg} \quad (5)$$

183 The coefficients C_1, C_2, C_3, C_4 and q_{Lavg} are expressed as

$$184 \quad C_1 = \frac{\Delta t - 2K^{j+1}\theta^{j+1}}{\Delta t + 2K^{j+1}(1 - \theta^{j+1})}$$

$$185 \quad C_2 = \frac{\Delta t + 2K^j\theta^j}{\Delta t + 2K^{j+1}(1 - \theta^{j+1})}$$

$$186 \quad C_3 = \frac{-\Delta t + 2K^j(1 - \theta^{j+1})}{\Delta t + 2K^{j+1}(1 - \theta^{j+1})}$$

$$187 \quad C_4 = \frac{2K\Delta t\Delta x}{\Delta t + 2K^{j+1}(1 - \theta^{j+1})}$$

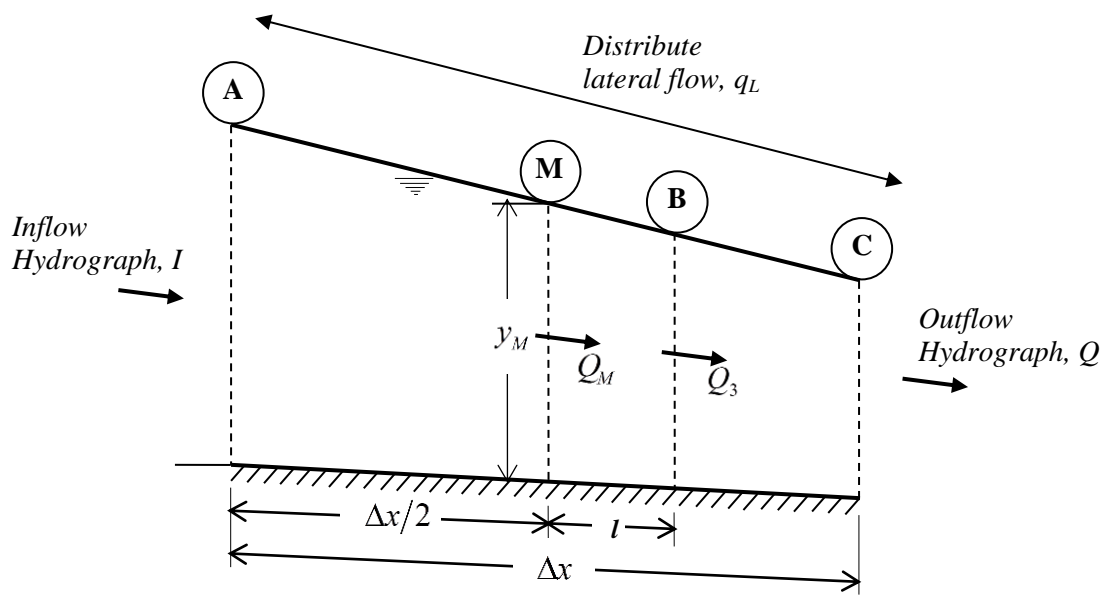
$$188 \quad q_{Lavg} = \frac{q_{L,j+1} + q_{L,j}}{2}$$

189 Considering the shape of lateral flow hydrograph as same as the inflow hydrograph, the
 190 lateral flow rate q_L joining to the river stretch (discharge per unit length of the channel) is
 191 obtained (Yadav et al., 2015) as

$$192 \quad q_L = \frac{I}{\sum_{i=1}^N I \Delta t} \times \frac{V_L}{L} \quad (6)$$

193 where, I is the inflow discharge at any time; L is the length of the river reach in meter; V_L is
 194 the volume of lateral flow .

195



196 **Fig: 1.** Concept diagram of VPMM method considering distributed lateral flow in river reach
 197
 198 (Yadav et al., 2015)

199 To calculate the discharge values at the downstream location, the VPMM method requires the
 200 following data- Manning's roughness value, Bed slope, River width (meter), Side slope and
 201 Cross-sectional shape. The method also requires river discharge data of the upstream gauging
 202 station and rainfall data to calculate the lateral flow of the intervening catchment. As the

203 VPMM method is a fully mass conservative, physically based method, it does not require any
 204 calibration. The precipitation and discharge data of year 2002 was used in simulation of the
 205 discharge at the downstream location.

206

207 **2.2 Support vector machine**

208 Vapnik et. al. (1995) proposed a kernel-based algorithm as support vector machine (SVM)
 209 which has a function form like physical models, however, the level of complexity is to be
 210 decided by the data used to train the model. The method was developed using the similar
 211 principle like ANN, however by using a novel way to approximate various functions (i.e.
 212 linear (LN), polynomial (PL), radial basis function (RBF), and sigmoid (SIG)) using the
 213 method of structural risk minimization (opposite to the empirical risk minimization). A kernel
 214 function is used to transform the data into higher dimensional feature space. The SRM
 215 principle allows the method to have a good generalization ability for the unseen data. Let
 216 $\{(x_1, y_1), \dots, (x_n, y_n)\}$ be assumed to be the given training data sets, where $x_i \in R^n$ represents
 217 the input sample space and $y_i \in R^l$ for $i = 1, \dots, l$ denotes respective target output, elements in
 218 the training data set represented by l . Error tolerance level is fixed by a value of ε (errors $< \varepsilon$
 219). The linear regression in SVM is estimated by solving the equation (7) as

$$220 \quad \text{Minimize } \frac{1}{2} \|w\|^2 + C \sum_{i=0}^n (\xi + \xi^*) \quad (7)$$

$$221 \quad \text{Subject to } \begin{cases} y_i - (w, x_i) - b \leq \varepsilon_i + \xi \\ (w, x_i) + b - y_i \leq \varepsilon_i + \xi^* \\ \xi_i, \xi_i^* \geq 0, i = 1, \dots, l \end{cases}$$

222 w denotes the normal vector, b is a bias, C represents a regularization constant, ε is the error
 223 tolerance level of the function, and the ξ, ξ^* are slack variables.

224 The support vector machine have variety of kernel function (mathematical function)
225 and its selection based on the problem at hand, which in turn has a direct impact on the
226 accuracy of the model (Yao et al., 2008). Various studies suggest that the RBF has higher
227 generalization ability and produce more accurate results than the other kernel types (Harpham
228 and Dawson, 2006; Yang et al., 2009; Tehrany et al., 2015, Yadav et al., 2017). A study by
229 Tehrany et al., (2014) suggested that RBF may produce less accurate results in case of longer
230 range extrapolation. However, RBF as a kernel function for SVM used by many researchers
231 in the past (Yu et al., 2004; Choy and Chan, 2003; Suryanarayana et al., 2014; Yadav et al.,
232 2016a, Yadav et al., 2017, Yadav et al., 2018) and has been found to be suitable for
233 simulation and prediction studies. RBF is defined as

$$234 \quad K(X_i, X_j) = \exp\left(-\gamma \|X_i - X_j\|^2\right) \quad (8)$$

235 where X_i and X_j are vectors in the input space, such as the vectors of features computed
236 from training and testing. γ is defined by, $\gamma = -\frac{1}{2\sigma^2}$ for which σ is the Gaussian noise level
237 of standard deviation.

238 The output of the SVM is critically dependent on the parameters such as regularization
239 constant (C) insensitive loss function (ε), and parameter of radial basis function (γ). Trial and
240 error procedure was used in the present study to optimize these parameters based on the
241 RMSE value. The trial continues by using different combinations of all three parameters till
242 the value of RMSE was minimized. Once the optimal parameters are obtained, the methods
243 requires time series of upstream and downstream gauging locations to simulate the discharge
244 values at the downstream location. The effect of lateral flow on the downstream discharge
245 values is automatically considered in the method as the lateral flow calculation is based on
246 the input and output discharge data. The time series data from the year 1999 to 2001 was used
247 for the training while the data from year 2002 was used for the testing.

248

249 **2.3 Wavelet analysis**

250 A wavelet analysis is based on Fourier analysis and was developed to analyze stationary and
251 non-stationary data. Wavelet decomposition is a technique used in case of non-periodic and
252 transient signals to extract the relevant time-frequency information by disintegrating the data
253 into low frequency and high frequency components. Wavelet decomposition breaks the signal
254 into low and high frequency components and utilizes the information hidden in the original
255 signal. The lower frequency components (approximation) are obtained using low pass filter
256 and captures the rapidly changing details of the signal. The higher frequency components
257 (details) are obtained using high pass filter to encompass the slowly changing features of the
258 signals. In this study, discrete wavelet transform (DWT) was used and the discharge time
259 series was decomposed into four resolution interval. Thus, some features of the subseries can
260 be seen more clearly than the original signal series. Though, DWT is able to decompose the
261 time series in many interval, it is important to note that higher number of resolution may also
262 slow down the computational speed. For each component a separate SVM model need to be
263 developed and the decomposed component may be given as the input for SVM. Later, the
264 output of the all the developed SVM (i.e. four in this case) will be summed to get the final
265 output in the form of recomposed time series.

266 There are two basic form of wavelet analysis, continuous wavelet transform (CWT) and
267 discrete wavelet transform (DWT). The continuous wavelet transform (CWT) of a signal $x(t)$
268 is defined as follows (Kalteh, 2013):

$$269 \quad CWT_x^\psi(\tau, s) = \frac{1}{\sqrt{|s|}} \int_{-\infty}^{+\infty} x(t) \psi^* \left(\frac{t-\tau}{s} \right) dt \quad (9)$$

270 where $\psi(t)$ is the mother wavelet function; s represents the scale parameter, τ is the
271 translation parameter.

272 The discrete wavelet transform (DWT) is defined as follows:

$$273 \quad \psi_{m,n}(t) = a^{-m/2} \psi\left(\frac{t - n\tau_0 a^m}{a^m}\right) \quad (10)$$

274 m and n is the resolution level and position which controls the scale and time; t is the time;
275 a is a specified fixed dilation step greater than 1; τ_0 is the location parameter that must be
276 greater than zero. The term $a^{-m/2}$ in the above equation normalizes the functions.

277 The two form of wavelet has been used in many studies, however it was observed that
278 the CWT is computationally costly and requires large number of data. On the other hand the
279 development and application of DWT is much simpler and easy to use (Adamowski and
280 Chan, 2011; Kalteh, 2013). Therefore, DWT has been used in this study where a father
281 wavelet function used for the extraction of low frequency components while the high
282 frequency component is extracted by using a complementary of the father wavelet, a mother
283 wavelet function. The decomposition of the data series is represented by the approximation
284 series A_m and the detail series D_m . Later, the both the approximation and detail series were
285 recomposed to get the final output of the model.

286 **2.4. Evaluation criteria**

287 The VPMM method was originally developed by Perumal and Price (2013) and further the
288 extended version considering the lateral flow was evaluated by Yadav et al., (2015). In the
289 flood forecasting study value of flood peak and its time of arrival is very important, hence in
290 this study three important evaluation criteria which is error in peak discharge (Q_{er}), error in
291 time to peak (t_{Qe}) and error in volume ($EVOL$) are adopted. The criteria for error in volume

292 has different definition than the one proposed by Perumal and Price (2013) as in their method
 293 the objective was to assess the error in mass conservation. However, in this study the lateral
 294 inflow from the intervening catchment is very significant hence the mass reproduction at the
 295 downstream location is bound to have higher value than the upstream location. Therefore,
 296 this study evaluated the volume reproduction ability of the selected methods based on the
 297 observed discharge at the downstream location. Further, the performance of VPMM, SVM
 298 and WA-SVM was also evaluated using the statistical indicators like root mean square error
 299 (RMSE), normalized mean square error (NMSE) and coefficient of determination (R^2). The
 300 aforementioned statistical indicator gives the interpretation about the overall reproduction
 301 ability of the selected models, and may not provide the information that how the model
 302 behaved throughout the flood event. Therefore, another evaluation criteria called absolute
 303 average relative error (AARE) was adopted to assess the model performance at each
 304 discharge ordinate. Furthermore, the performance of the selected methods was also evaluated
 305 using graphical analysis where the closeness with which the proposed method reproduces the
 306 benchmark solution, including the closeness of shape and size of the hydrograph, can be
 307 measured using the Nash–Sutcliffe (NSE) efficiency criterion. The definition of RMSE,
 308 NMSE, NSE and R^2 can be found easily in the literature, however the definition for some of
 309 the specific performance measures are given as follows:

310 Error in peak discharge (Q_{er})

$$311 \quad Q_{er} = \left(\frac{Q_s}{Q_o} - 1 \right) \times 100 \quad (11)$$

312 Relative error in time to peak (t_{Qe})

$$313 \quad t_{Qe} = t_{Qs} - t_{Qo} \quad (12)$$

314 Error in volume (*EVOL*)

315
$$EVOL = \left[\left\{ \frac{\sum_{i=1}^N Q_{si}}{\sum_{i=1}^N Q_{oi}} \right\} - 1 \right] \times 100 \quad (13)$$

316

317

318 Absolute average relative error (AARE)

319
$$AARE = \frac{1}{N} \sum_{i=1}^N \left| \frac{Q_{oi} - Q_{si}}{Q_{si}} \right| \times 100 \quad (14)$$

320 where Q_{er} represents the percentage error in simulated peak discharge; Q_s is the simulated
321 peak discharge of the flood event at the downstream location (m^3/s); Q_o is the observed peak
322 discharge of the flood event at the downstream location (m^3/s); t_{Q_e} is the relative error in
323 time to peak of the simulated flood event (hr); t_{Q_s} time to peak of the simulated flood event
324 (hr); t_{Q_o} time to peak of the observed flood event (hr); *EVOL* is the error in volume is
325 simulated flood event (%); Q_{si} is the *i*th ordinate of the simulated flood event (m^3/s); Q_{oi} is the
326 *i*th ordinate of the observed flood event (m^3/s) and *N* is the total number of ordinates in the
327 flood event.

328 **2.5 Evaluation of model complexity**

329 The level of complexity of a specific model is tested using Akaike information criterion
330 (AIC) and model selection criteria (MSC). The most appropriate model based on the model
331 complexities is the one with the smallest values of the AIC and largest value of MSC. The
332 performance measures are also defined as;

333
$$AIC = N \ln \left[\sum_{i=1}^N (Q_{oi} - Q_{si})^2 \right] + 2N_p \quad (15)$$

334
$$MSC = \ln \left[\frac{\sum_{i=1}^N (Q_{oi} - \bar{Q}_s)}{\sum_{i=1}^N (Q_{oi} - Q_{si})} \right] - \frac{2N_p}{N} \quad (16)$$

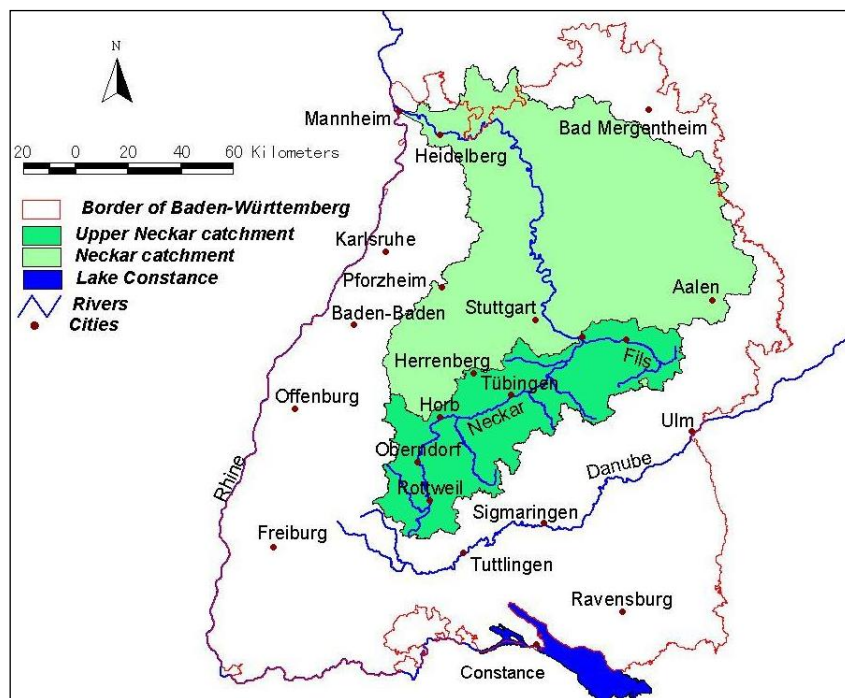
335 where \bar{Q}_s represents the average simulated discharge and N_p represents the number of model
 336 parameters.

337

338 **3. Study area and data**

339 The research work as a part of this study was mainly performed on a part of the Neckar River
 340 basin (Fig.2). This region is situated in the South- Western part of Germany in the state of
 341 Baden Württemberg. The river in the catchment is unaffected by large hydropower
 342 generation plants and other such water management structures or navigational reasons, which
 343 are the most common reasons influencing the runoff characteristics of the catchment area.
 344 The study area of this research is characterised by strong differences in altitude between the
 345 foothills of the Black Forest in the west, the valley of the Neckar in the centre and once again
 346 the steep ascent to the Schwäbische Alb in the east. The catchment consists of lots of narrow
 347 valleys. There is a wide variety of vegetation in the study catchment. In the western part of
 348 the catchment the soil is acidic and poor in minerals which supports only Spruce, fir and
 349 beech trees. The same forest is also found in the sandy soil of Keuper. The pasture, meadows,
 350 fruits, vines, ash tress, elm and lime trees are also found in the smaller pockets. The study
 351 was conducted between the two initial observation stations Rottweil and Oberndorf on the
 352 Neckar River. Distance between two stations is 24.2 km. The intermediate drainage area
 353 between two stations is 235 km² which is around 34 % of the total drainage area of Oberndorf

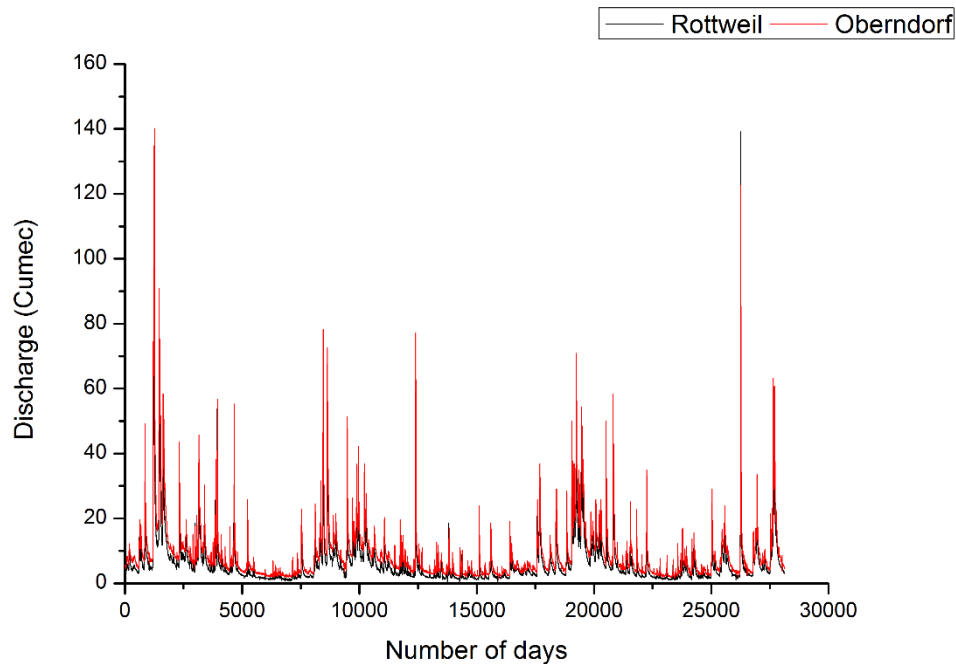
354 gauging station. The hourly amounts of precipitation used in the VPMM for the period from
 355 1999 to 2002 are obtained from 3 precipitation stations which are distributed in and around
 356 the catchment area. The data based modeling (SVM and WA-SVM) is based only on the
 357 discharge time series from 1999 to 2002 (Fig. 3) which was provided by the University of
 358 Stuttgart, Germany. The description of the study area is partly based on the description of
 359 Das (2006) and CCHYDRO (1999). The discharge time series from 1999-2001 was used for
 360 the training and, nine flood events from the year 2002 are selected for the comparative
 361 analysis of the selected methods. The event selection was completely random but keeping in
 362 mind that the peak discharge value should be high and lateral flow contribution must be more
 363 than 10% in all events. The parameters for the application of extended VPMM were taken
 364 from the study of Yadav et al., (2015).



365

366

Fig.2 Neckar catchment (IWS, Stuttgart)



367

368 **Fig. 3** Time series at Rottweil (upstream) and Oberndorf (downstream) gauging stations

369 **4. Results and discussions**

370 **4.1 Flood Routing Using VPMM, SVM and WA-SVM**

371 The extended VPMM method and its parameters were obtained from the study conducted by
 372 Yadav et al., (2015) for the same river stretch. The VPMM method under consideration has
 373 only two parameters K and θ which depends on the cross sectional information and the flow
 374 characteristics. The routing reach information such as bed slope and Manning's roughness
 375 value were obtained from the study reports of the Neckar river catchment, But the bed width
 376 and side slope of the cross section (Table 1) of the channel reach is optimized by the ROPE
 377 algorithm (Singh, 2008, Yadav et al., 2015). To avoid the influence of lateral inflow on the
 378 parameter optimization process the flood event with a minimum lateral flow among the 9
 379 events is considered for the analysis. The data based model namely SVM and WA-SVM were
 380 developed using LIBSVM toolbox (Chang et al. 2011) to predict the discharge at the
 381 downstream location. The Radial Basis Function was adopted as kernel function for SVM
 382 and its parameters C and γ were obtained using a trial and error procedure where the trial

383 continues till the value of RMSE was minimized. Later, the SVM model was suitability
 384 coupled with wavelet analysis (WA) which decomposes the input discharge time series using
 385 DWT into approximation and detailed time series (Fig. 4). The parameters for SVM and WA-
 386 SVM has been presented in Table 2. After the model calibration (VPMM) or training (SVM,
 387 WA-SVM) they were used to predict the discharge hydrograph of 9 flood events of the year
 388 2002.

389 **Table 1.** Parameters for the development of VPMM method

Parameter	Value
Manning's roughness	0.035
Bed slope	0.0034
River width (meter)	8.417
Side slope	1.035
Cross-sectional shape	Trapezoidal

390

391 **Table 2.** Optimal SVM and WA-SVM parameters for various decomposition series

Model	Decomposed series	best C	best γ
SVM		3.104	0.0412
WA-SVM	Approximation series	42	0.0611
	D1 series	3	0.0412
	D2 series	3	0.0712
	D3 series	7	0.0912
	D4 series	9	0.0812

392

393 Table 3 presents the statistical analysis of the simulated hydrograph obtained by VPMM,
 394 SVM and WA-SVM. The VPMM reproduced 7 out of 9 flood events with highest accuracy,
 395 where the error measures like NMSE, RMSE values ranges between 0.018 to 0.083 and 1.471

396 (m³/s) to 4.301 (m³/s), respectively. Similarly the values for R² and NSE ranges between
397 0.968 to 0.997 and 0.872 to 0.982, respectively. In case of SVM, the values obtained for
398 NMSE and RMSE were significantly high for most of the flood events and ranges between
399 0.046 to 0.176 and 2.932 (m³/s) to 5.918 (m³/s), respectively. The fitness criteria (R² and
400 NSE) also follows the similar trend like error measures and ranges between 0.831 to 0.966
401 and 0.822 to 0.954, respectively. The inclusion of wavelet analysis has definitely improved
402 the accuracy of SVM and outperforms it in all flood events except 1, 3 and 9. Though, it is
403 evident from the statistical analysis that the VPMM method shows superiority over SVM and
404 WA-SVM, the reproduction of the downstream hydrographs for all the flood events by the
405 data based models are very close to the observed hydrographs. This argument is well
406 supported by the graphical representation of the observed and simulated hydrographs by
407 VPMM, SVM and WA-SVM (Fig. 5-13). It is also evident from these figures that the
408 absolute average relative error (AARE) of VPMM is very low. The AARE of SVM and WA-
409 SVM is significantly higher than the VPMM, however WA-SVM shows relatively less error
410 than the SVM. These figures reveal that, under significant lateral flow conditions, the rising
411 limb, recession limb, and the peaks of the event-based flood hydrographs are all most well-
412 reproduced by the VPMM, SVM and WA-SVM model.

413 **Table. 3** Performance of VPMM, SVM and WA-SVM during the discharge prediction at the
414 Oberndorf gauging station

Flood event	Method	NMSE	R ²	RMSE (m ³ /s)	NSE
1	VPMM	0.028	0.984	3.421	0.948
	SVM	0.049	0.966	3.316	0.951
	WASVM	0.052	0.962	3.434	0.948
2	VPMM	0.083	0.980	4.197	0.916
	SVM	0.130	0.922	5.244	0.869
	WASVM	0.118	0.928	5.009	0.881
3	VPMM	0.018	0.987	2.195	0.982
	SVM	0.129	0.948	5.918	0.870

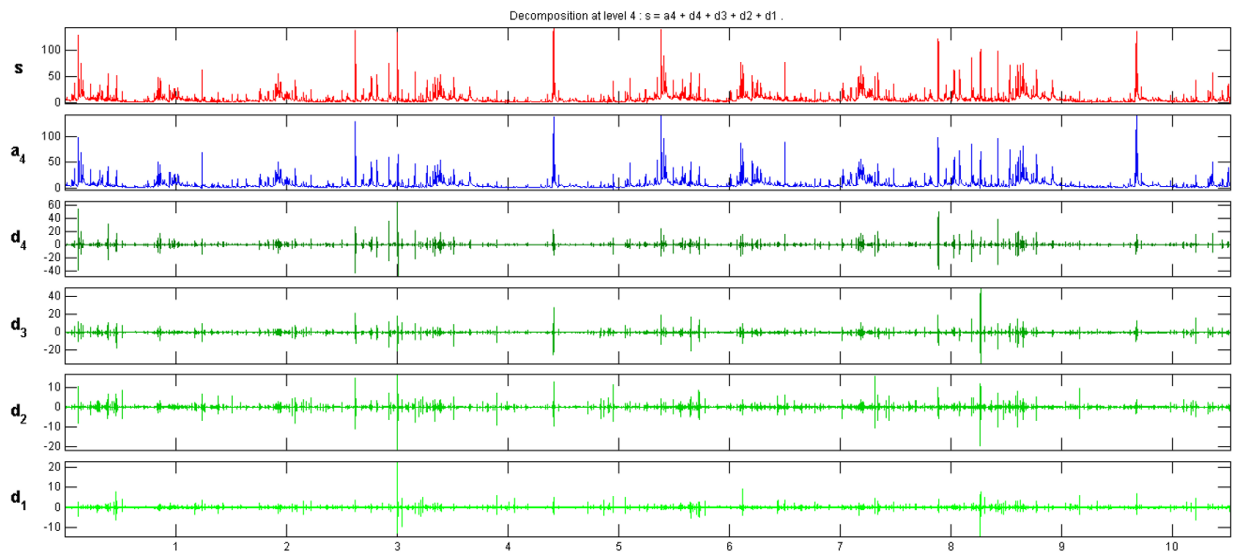
	WASVM	0.145	0.943	6.261	0.855
4	VPMM	0.020	0.981	1.471	0.979
	SVM	0.176	0.831	4.356	0.822
	WASVM	0.175	0.835	4.345	0.823
5	VPMM	0.071	0.968	4.301	0.928
	SVM	0.106	0.919	5.254	0.893
	WASVM	0.099	0.926	5.061	0.901
6	VPMM	0.030	0.987	2.415	0.970
	SVM	0.081	0.951	4.005	0.919
	WASVM	0.069	0.958	3.694	0.931
7	VPMM	0.035	0.970	3.579	0.965
	SVM	0.046	0.954	4.106	0.954
	WASVM	0.046	0.954	4.093	0.954
8	VPMM	0.128	0.976	4.545	0.872
	SVM	0.053	0.953	2.932	0.947
	WASVM	0.053	0.955	2.920	0.947
9	VPMM	0.015	0.997	1.469	0.985
	SVM	0.062	0.964	3.011	0.938
	WASVM	0.070	0.955	3.191	0.929

415

416

417 Further analysis of the results indicates that the VPMM model works well in both the cases of
418 single or multi-peak peak flood events, however, data based models simulates the multi-peak
419 flood events (Events 1 and 8) better than VPMM. The reason for such outcome can be
420 attributed to the fact that the data based model performance primarily depends on the data
421 length. In case of flood event 8, the discharge time series length is around 800 hrs with
422 multiple peaks, which allowed the model to learn such occurrence properly. The study
423 suggest that, if the data based models are fed with sufficient length of discharge time series
424 data which encompass the variability in nature, they can simulate the discharge process with
425 reasonable accuracy. On the other hand, the reduction in accuracy of VPMM for these flood
426 events derives from the uncertainty in estimating the lateral flow which, mainly depends on
427 the initial soil moisture conditions. The spatial and temporal variability of soil moisture

428 content can have significant impact on the lateral flow estimation which in turn will reflect in
429 the simulation accuracy of the VPMM.

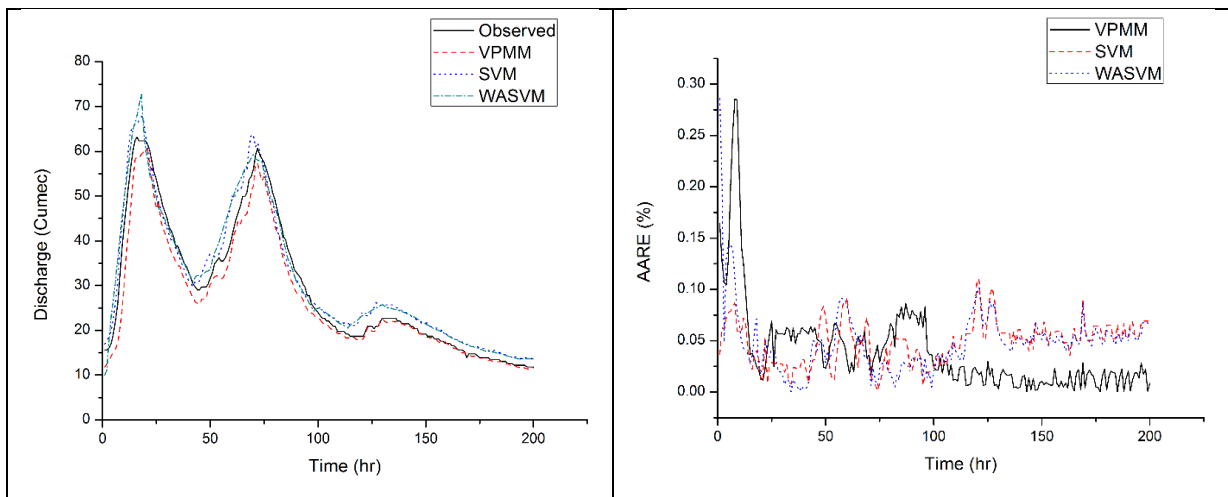


430

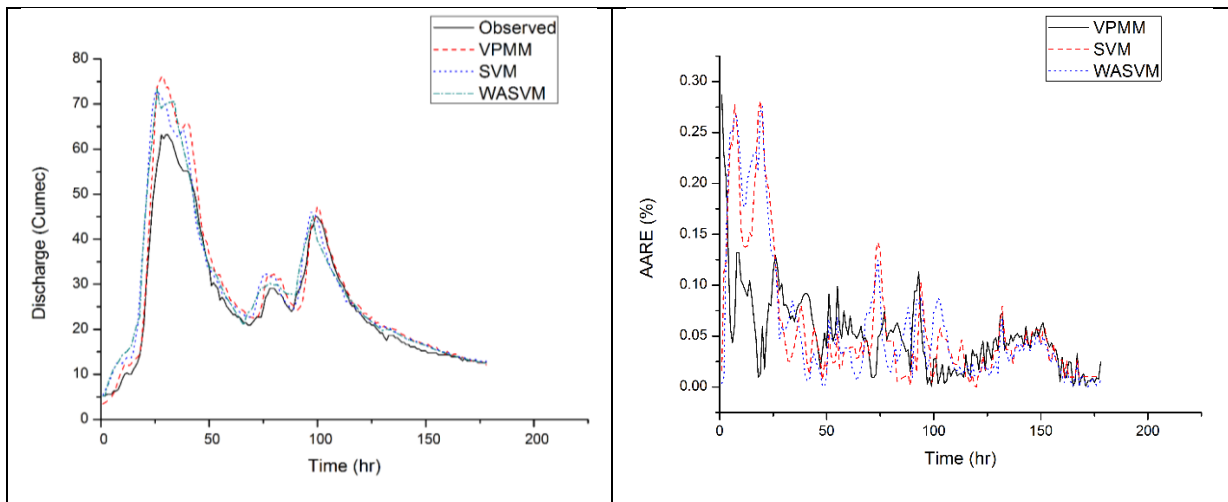
431 **Fig. 4** Decomposed time series of the for the period of 1999 to 2000

432

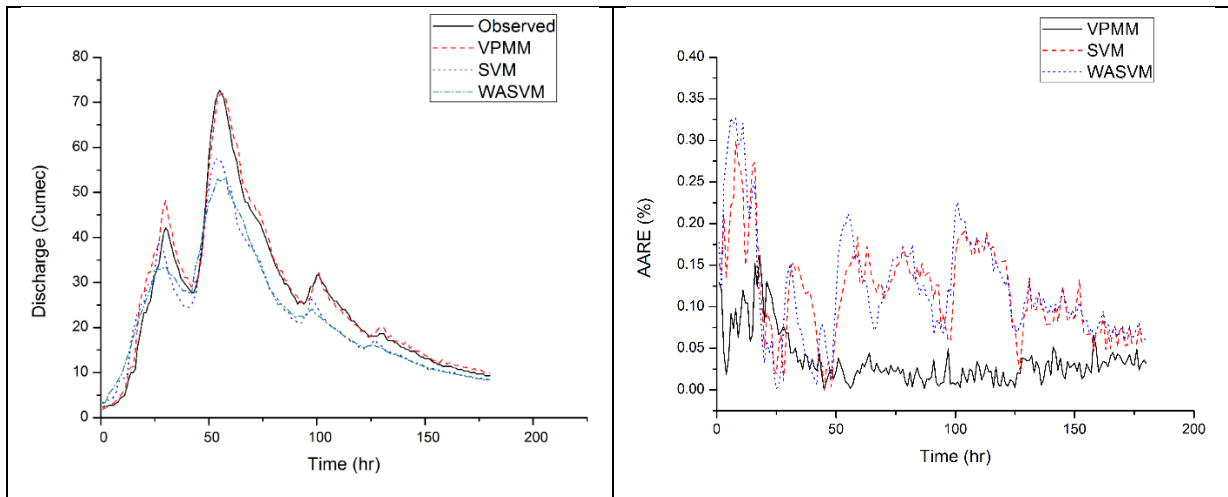
433



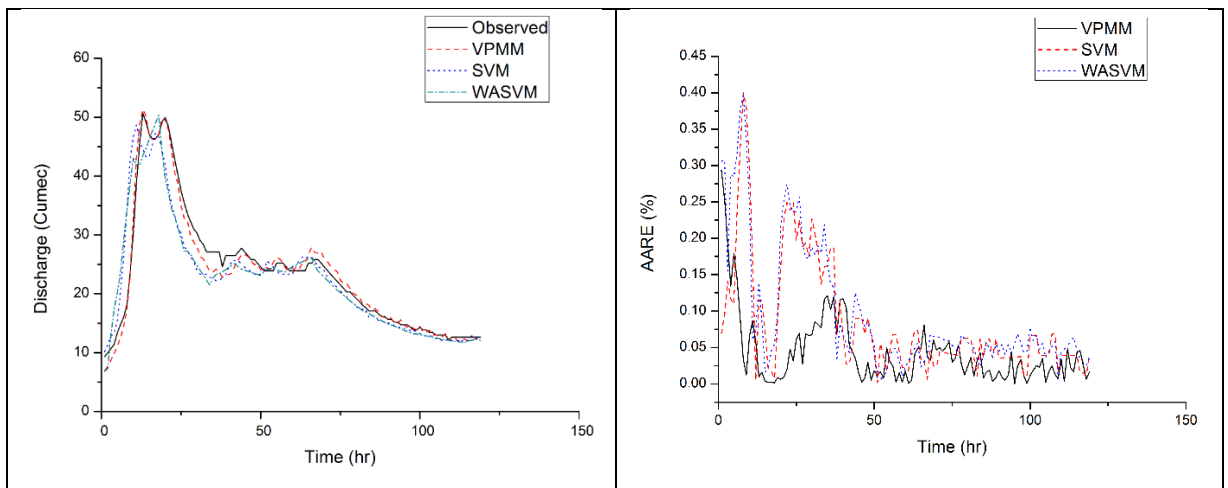
434 **Fig. 5** Routed hydrograph and AARE for flood event 1 using VPMM, SVM and WASVM.



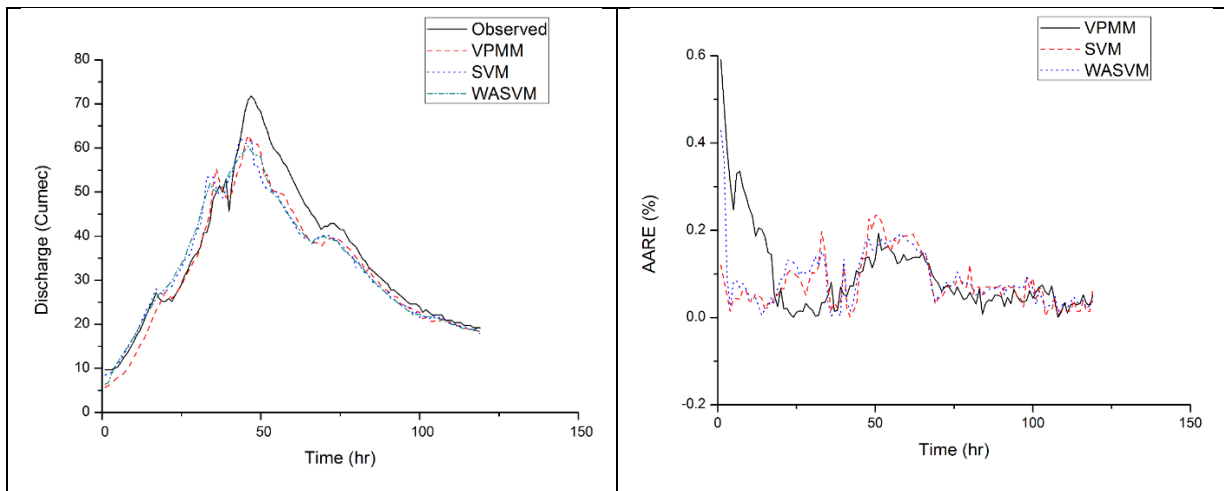
435 **Fig. 6** Routed hydrograph and AARE for flood event 2 using VPMM, SVM and WASVM.



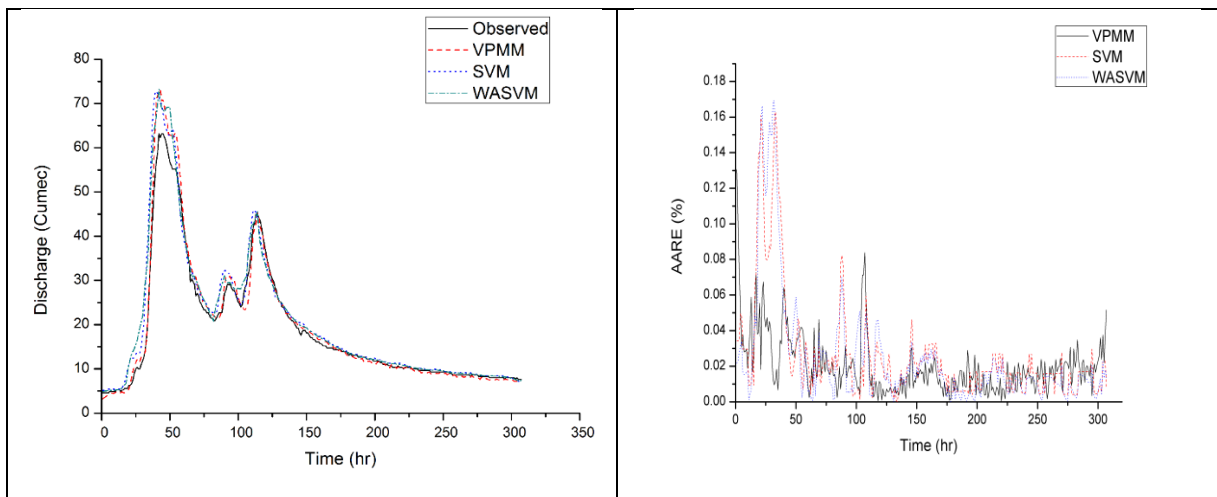
436 **Fig. 7** Routed hydrograph and AARE for flood event 3 using VPMM, SVM and WASVM.



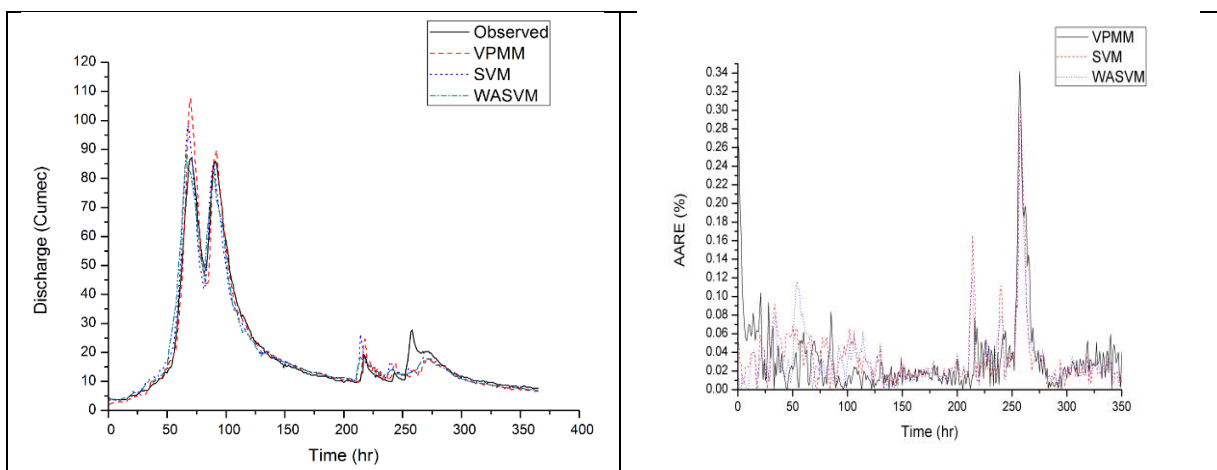
437 **Fig. 8** Routed hydrograph and AARE for flood event 4 using VPMM, SVM and WASVM.



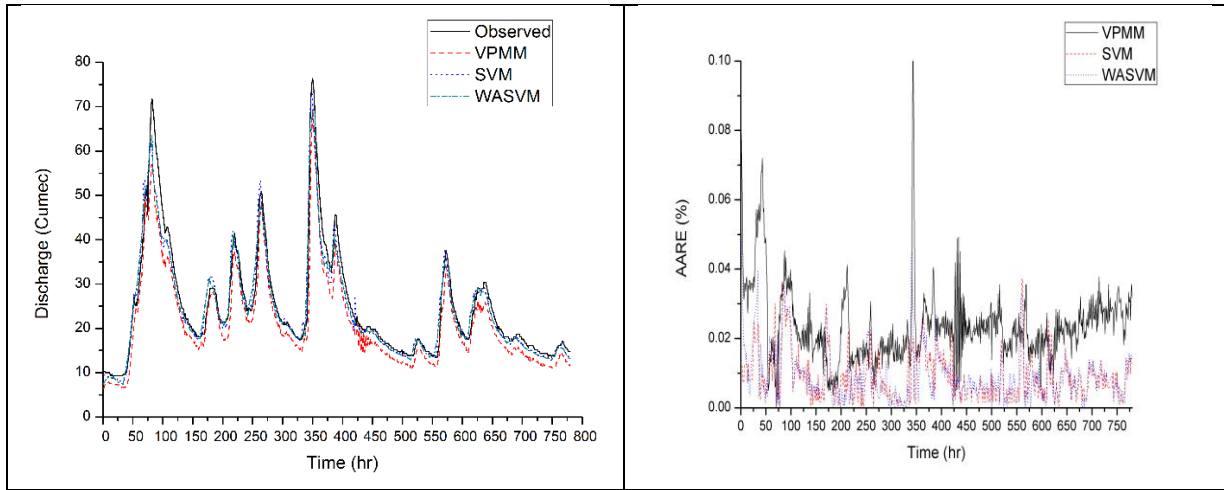
438 **Fig. 9** Routed hydrograph and AARE for flood event 5 using VPMM, SVM and WASVM.



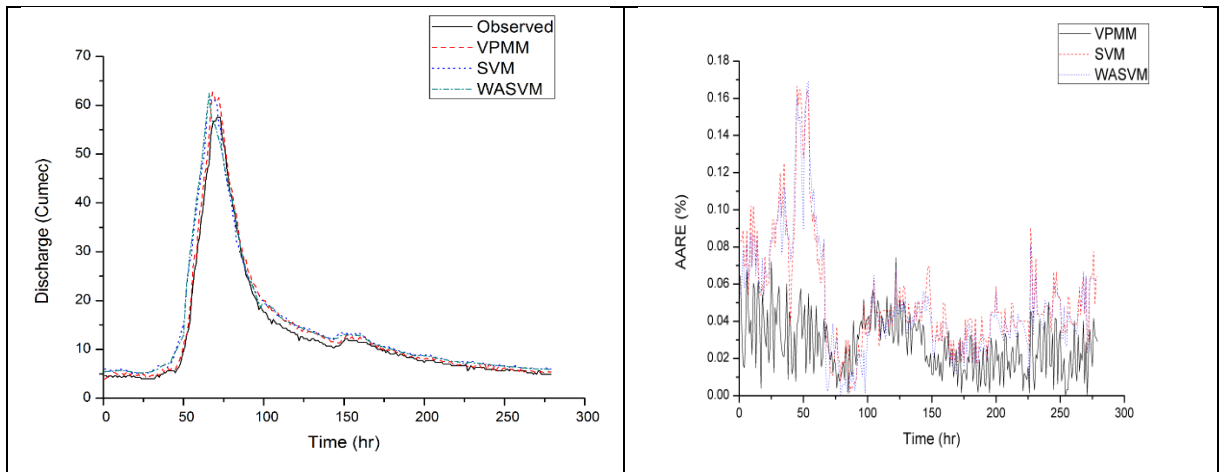
439 **Fig. 10** Routed hydrograph and AARE for flood event 6 using VPMM, SVM and WASVM.



440 **Fig. 11** Routed hydrograph and AARE for flood event 7 using VPMM, SVM and WASVM.



441 **Fig. 12** Routed hydrograph and AARE for flood event 8 using VPMM, SVM and WASVM.

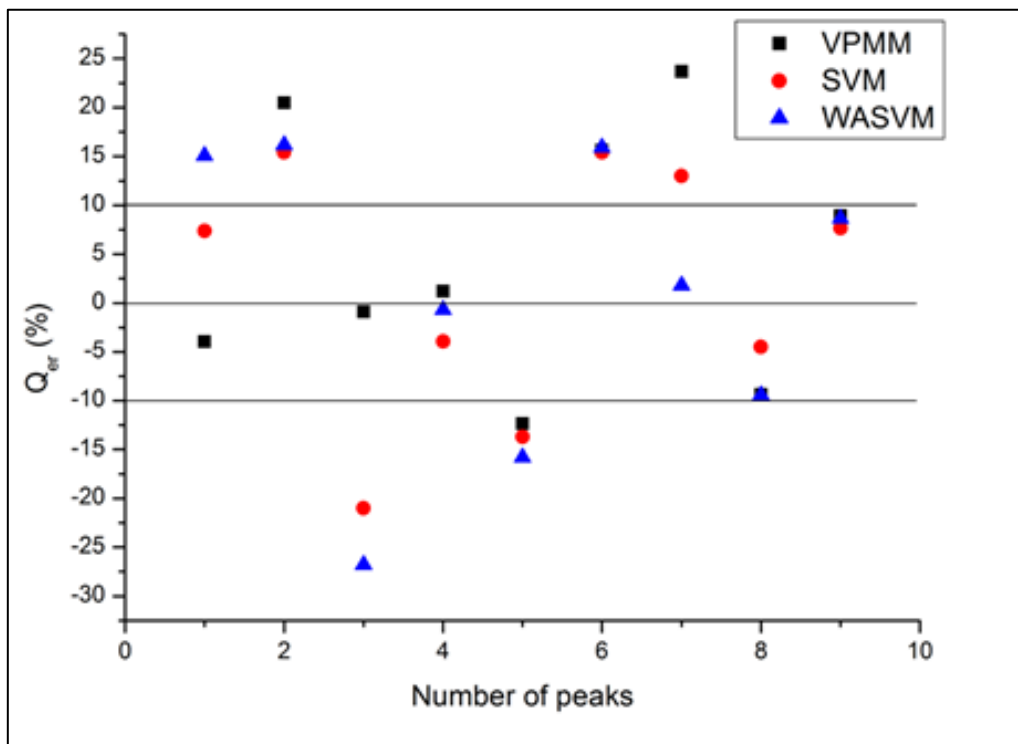


442 **Fig. 13** Routed hydrograph and AARE for flood event 9 using VPMM, SVM and WASVM.

443

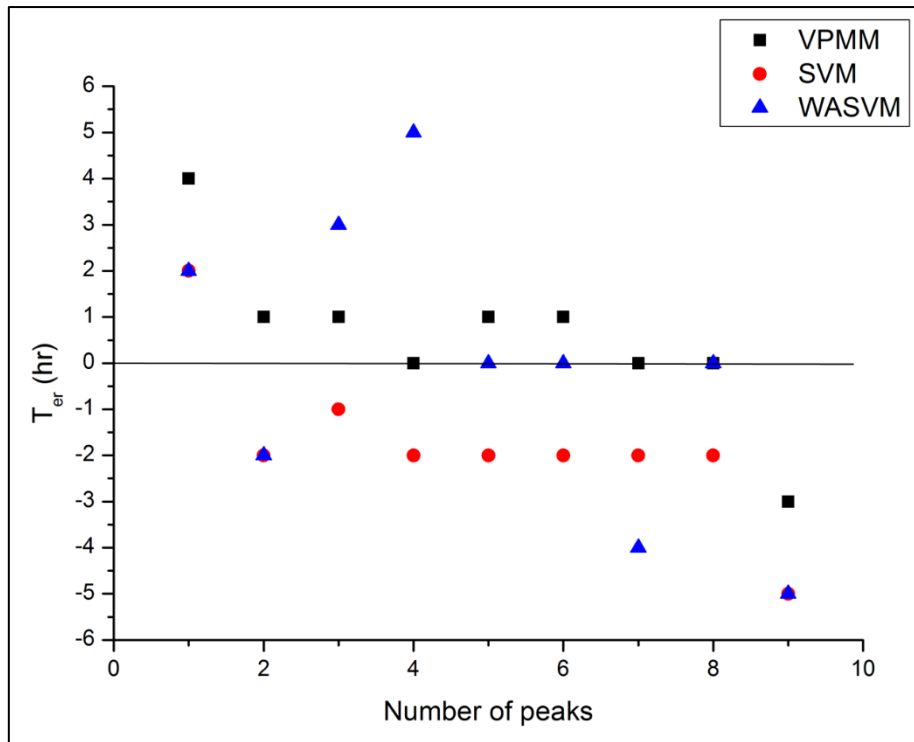
444 Further, considered methods in this study were also evaluated using the original criteria used
 445 for the development of VPMM. The percentage error in the peak discharge (Q_{er} in %), the
 446 error in the time-to-peak discharge (t_{Qe} in hr), and the percentage error in the volume ($EVOL$
 447 in %) for all the 9 flood events has been depicted in Figs. 14, 15 and 16. It is evident from the
 448 Fig. 14 that the VPMM method predicts most of the peak values (5 out of 9) within $\pm 10\%$
 449 error and just 2 above the 20% error. However, in case of SVM and WA-SVM Q_{er} is well
 450 above the $\pm 10\%$ range for most of the flood events. Which suggest that the data based
 451 models may requires more training to predict such high discharge values which comes rarely

452 in a discharge time series but extremely important in case of flood forecasting. Similarly, Fig.
 453 15 presents the error in time to peak discharge and VPMM predicts the peak value very close
 454 to its time of arrival in observed flood event. In fact, 7 out of 9 peaks has error 1 hour or less,
 455 and just two with the error range of ± 4 (hr). SVM also produced most of the peak discharge
 456 values with ± 2 (hr) error, however WA-SVM shows the higher error variation ranging from
 457 -2 to $+2$ (hr). Further, the percentage error in the volume (*EVOL* in %) is depicted in Fig.
 458 16, which shows that the VPMM method despite receiving significant amount of lateral flow
 459 from the intervening catchment could reproduce the downstream hydrograph with just
 460 $\pm 10\%$ error in volume for 8 out of 9 flood events. Though, the error in the volume for SVM
 461 and WA-SVM is also within the same range as it was for the VPMM, however some flood
 462 events showed higher error.



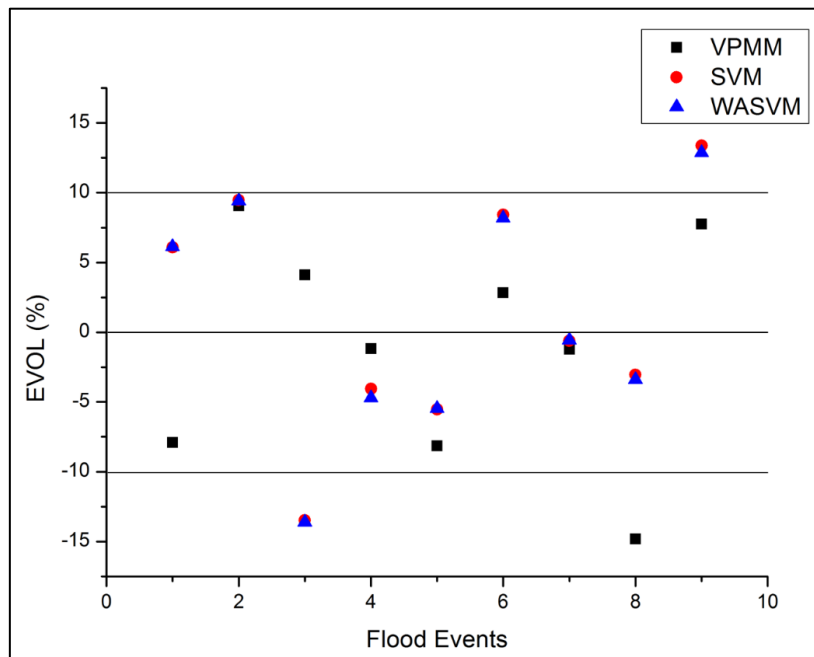
463
 464
 465

Fig. 14 Error in peak discharge prediction while using VPMM, SVM and WASVM



466

467 **Fig. 15** Error in time to peak discharge prediction while using VPMM, SVM and WASVM



468

469 **Fig. 16** variation of error in volume while using VPMM, SVM and WASVM

470

471 **4.2 Level of Complexity in VPMM, SVM and WA-SVM**

472 The method under consideration were also evaluated to assess the level of complexity while
 473 desgining the model for discharge prediction. Table 4 presents the model complexity analysis
 474 of VPMM, SVM and WA-SVM based on the number of parameter each model requires to be
 475 tuned while designing the model for a specific application. The VPMM method has only two
 476 parameters that is K and θ while the SVM has three parameters namely regularization
 477 constant (C), insensitive loss function (ϵ), and parameter of radial basis function (γ). It is
 478 evident from the table that the Akaike information criterion (AIC) is lowest while using
 479 VPMM, in comparison to SVM and WASVM for most of the flood events. Similarly the
 480 model selection criteria (MSC) value is highest for 8 out of 9 flood events when VPMM is
 481 used, however it decreased significantly for SVM and WA-SVM.

482

483 **Table 4.** Akaike information criterion (AIC) and model selection criteria (MSC) for VPMM,
 484 SVM and WA-SVM

Flood Event	AIC			MSC		
	VPMM	SVM	WA-SVM	VPMM	SVM	WA-SVM
1	1555.64	1545.19	1559.21	-0.02	-0.030	-0.030
2	1437.02	1518.28	1501.94	-0.022	-3.203	-5.220
3	1221.69	1580.78	1601.07	-0.022	0.233	-4.822
4	664.62	924.92	924.34	-0.033	-0.391	-2.030
5	919.94	969.57	960.66	-0.033	-0.805	-4.307
6	2303.60	2616.07	2566.52	-0.013	-0.610	-3.529
7	3088.30	3190.54	3188.27	-0.011	-0.040	-2.250
8	7560.23	6878.02	6871.93	-0.005	1.348	-2.286
9	1789.87	2192.25	2224.57	-0.014	-0.889	-3.288

485

486

487 **5. Conclusion**

488 In this study two approaches were used to predict the downstream discharge of Neckar River
489 in which VPMM is a physically based method and the SVM is data based method. Further,
490 wavelet analysis was also used to develop a hybrid WA-SVM model. The study was
491 conducted using 9 flood events from the year 2002 which is characterised of having
492 significant lateral flow joining from the intervening catchment, which in general is difficult to
493 model due to its spatial and temporal variability. Based on the analysis of statistical and
494 graphical results, it is inferred that the extended physically based variable parameter
495 Muskingum routing method (VPMM) is more robust and reliable than the data based models
496 like SVM and WA-SVM, when used to predict the discharge in a river reach with significant
497 lateral flow joining between the upstream and downstream gauging stations. However, it is
498 also evident from the analysis that the data based models successfully captured the flood
499 wave moment phenomenon and were able to map the process even with lateral flow, hence
500 reproduced the discharge hydrograph close to the observed hydrograph at the downstream
501 location. Further, based on the Akaike information criterion (AIC) and model selection
502 criteria (MSC), it can be concluded that the VPMM model is relatively less complex than the
503 SVM and WA-SVM. Lastly, it can be summarised that the physically based extended VPMM
504 method can predict the discharge hydrograph better than the data based mode, however, in
505 case of multi-peak flood events with sufficient discharge data, the later performed better than
506 VPMM method.

507

508 **Acknowledgement**

509 The author thankfully acknowledge the support and motivation provided by Prof. M.
510 Perumal. The necessary data to conduct this study was provided by TU Stuttgart, Germany.
511 The financial support to conduct this study was provided by IIT Delhi, India.

512

513 **Conflict of Interest Statement**

514 We confirm that this manuscript has not been published elsewhere and is not under
515 consideration by another journal. All the authors have approved the manuscript and agree
516 with the submission to Neural Computing and Applications Journal. The financial support
517 was provided by IIT Delhi. The authors have no conflict of interest to declare.

518 **References**

519 Adamowski, J., & Sun, K., 2010. Development of a coupled wavelet transform and neural
520 network method for flow forecasting of non-perennial rivers in semi-arid watersheds. *Journal*
521 *of Hydrology*, 390(1), 85-91.

522

523 Adamowski, J., & Chan, H. F., 2011. A wavelet neural network conjunction model for
524 groundwater level forecasting. *Journal of Hydrology*, 407(1), 28-40.

525

526 ASCE Task Committee on Application of Artificial Neural Networks in Hydrology, 2000.

527

528 Agarwal, A., Maheswaran, R., Kurths, J., & Khosa, R. 2016. Wavelet Spectrum and self-
529 organizing maps-based approach for hydrologic regionalization-a case study in the western
530 United States. *Water Resources Management*, 30(12), 4399-4413.

531

532 Badrzadeh, H., Sarukkalige, R., & Jayawardena, A. W., 2013. Impact of multi-resolution
533 analysis of artificial intelligence models inputs on multi-step ahead river flow forecasting.
534 *Journal of Hydrology*, 507, 75-85.

535

536 Beven, K., 2006. A manifesto for the equifinality thesis. *Journal of hydrology*, 320(1), 18-36.
537 CC-HYDRO, 1999. Impact of Climate Change on River Basin Hydrology under Different
538 Climatic Conditions, March 1999. Universität Stuttgart, Germany.

539

540 Borges, R. V., Garcez, A. D. A., & Lamb, L. C., 2011. Learning and representing temporal
541 knowledge in recurrent networks. *IEEE Transactions on Neural Networks*, 22(12), 2409-
542 2421.

543

544 Cannas, B., Fanni, A., See, L., & Sias, G., 2006. Data preprocessing for river flow forecasting
545 using neural networks: wavelet transforms and data partitioning. *Physics and Chemistry of the*
546 *Earth* 31 (18), 1164–1171.

547

548 Chang C. C., & Lin C. J., 2011. LIBSVM: a library for support vector machines. *ACM Trans.*
549 *Intell. Syst. Technol.* 2 (3) 27.

550

551 Chow, V.T., Maidment, D.R., & Mays, L.W., 1988. *Applied Hydrology*. McGraw-Hill, New
552 York.

553

554 Choy K., & Chan C., 2003. Modelling of river discharges and rainfall using radial basis
555 function networks based on support vector regression, *Int. Journal of System Science*, 34 (1)
556 763–773

557

558 Das, T., 2006. *The Impact of Spatial Variability of Precipitation on the Predictive*
559 *Uncertainty of Hydrological Models*, Ph.D. Dissertation No. 154, University of Stuttgart.

560

561 Dawson C.W., & Wilby R., 1998. An artificial neural network approach to rainfall–runoff
562 modeling. *Hydrological Sciences Journal*, 43 (1), pp. 47–66.

563

564 Ghalkhani, H., Golian, S., Saghafian, B., Farokhnia, A., & Shamseldin, A., 2013. Application
565 of surrogate artificial intelligent models for real-time flood routing. *Water and Environment*
566 *Journal*, 27(4), 535-548.

567

568 Harpham, C., & Dawson, C. W., 2006. The effect of different basis functions on a radial basis
569 function network for time series prediction: a comparative study. *Neurocomputing*, 69(16),
570 2161-2170.

571

572 Kalteh, A. M., 2013. Monthly River flow forecasting using artificial neural network and
573 support vector regression models coupled with wavelet transform. *Computers &*
574 *Geosciences*, 54, 1-8.

575

576 Karahan, H., Gurarslan, G., & Geem, Z. W., 2015. A new nonlinear Muskingum flood
577 routing model incorporating lateral flow. *Engineering Optimization*, 47(6), 737-749.

578
579
580
581
582
583
584
585
586
587
588
589
590
591
592
593
594
595
596
597
598
599
600
601
602
603
604
605
606
607
608
609
610
611

Kasiviswanathan, K. S., He, J., Sudheer, K. P., & Tay, J. H., 2016. Potential application of wavelet neural network ensemble to forecast streamflow for flood management. *Journal of Hydrology*, 536, 161-173

Kisi, O., 2008. River flow forecasting and estimation using different artificial neural network techniques. *Hydrological Research*, 39 (1), 27–40.

Koza, J. R., 1992. *Genetic programming: on the programming of computers by means of natural selection* (Vol. 1). MIT press.

Lin, T., Guo, T., & Aberer, K., 2017. Hybrid neural networks for learning the trend in time series. In *Proceedings of the Twenty-Sixth International Joint Conference on Artificial Intelligence, IJCAI-17* (pp. 2273-2279).

Loague, K., & VanderKwaak, J. E., 2004. Physics-based hydrologic response simulation: Platinum bridge, 1958 Edsel, or useful tool. *Hydrological Processes*, 18(15), 2949-2956.

Maier, H. R., & Dandy, G. C., 2000. Neural networks for the prediction and forecasting of water resources variables: a review of modelling issues and applications. *Environmental modelling & software*, 15(1), 101-124.

McCarthy, G.T., 1938. The unit hydrograph and flood routing. In: *Conference of North Atlantic Div., U.S. Army Corps of Engineers*.

Nourani, V., Baghanam, A. H., Adamowski, J., & Kisi, O., 2014. Applications of hybrid wavelet–Artificial Intelligence models in hydrology: A review. *Journal of Hydrology*, 514, 358-377.

O'Donnell, T., 1985. A direct three-parameter Muskingum procedure incorporating lateral inflow. *Hydrological Science Journal*. 30 (4), 479–496.

Nayak, P. C., Sudheer, K. P., & Jain, S. K., 2007. Rainfall-runoff modeling through hybrid intelligent system. *Water Resources Research*, 43(7).

612 Perumal, M., 1994a. Hydrodynamic derivation of a variable parameter Muskingum method:
613 1. Theory and solution procedure. *Hydrological sciences journal*, 39(5), 431-442.
614

615 Perumal, M., 1994b. Hydrodynamic derivation of a variable parameter Muskingum method:
616 2. Verification. *Hydrological sciences journal*, 39(5), 443-458.
617

618 Perumal, M., O'Connell, P.E., & Ranga Raju, K.G., 2001. Field applications of a variable
619 parameter Muskingum method. *Journal of Hydraulic Engineering*. 6 (3), 1084-0699/01/0003-
620 0196-0207.
621

622 Perumal, M., & Sahoo, B., 2008. Volume conservation controversy of the variable parameter
623 Muskingum–Cunge method. *Journal of Hydraulic Engineering*, 134(4), 475-485.
624

625 Perumal, M., & Price, R.K., 2013. A fully volume conservative variable parameter
626 McCarthy-Muskingum method: theory and Verification. *Journal of Hydrology*. 502, 89–102.
627

628 Perumal, M., Tayfur, G., Rao, C. M., & Gurarslan, G., 2017. Evaluation of a physically based
629 quasi-linear and a conceptually based nonlinear Muskingum methods. *Journal of*
630 *Hydrology*, 546, 437-449.
631

632 Ponce, V. M., & Yevjevich, V., 1978. Muskingum-Cunge method with variable parameters.
633 *Journal of the Hydraulics Division*, 104(12), 1663-1667.
634

635 Price, R. K., 2009. Volume-conservative nonlinear flood routing. *Journal of Hydraulic*
636 *Engineering*, 135(10), 838-845.
637

638 Rezaeianzadeh, M., Tabari, H., Yazdi, A. A., Isik, S., & Kalin, L., 2014. Flood flow
639 forecasting using ANN, ANFIS and regression models. *Neural Computing and Applications*,
640 25(1), 25-37.
641

642 Sang, Y. F., 2013. A review on the applications of wavelet transform in hydrology time series
643 analysis. *Atmospheric research*, 122, 8-15.
644

645 Shiri, J., & Kisi, O., 2010. Short-term and long-term streamflow forecasting using a wavelet
646 and neuro-fuzzy conjunction model. *Journal of hydrology*, 394(3), 486-493.

647

648 Shiri, J., Kişi, Ö., Makarynskyy, O., Shiri, A. A., & Nikoofar, B., 2012. Forecasting daily
649 stream flows using artificial intelligence approaches. *ISH Journal of Hydraulic Engineering*,
650 18(3), 204-214.

651

652 Singh, S.K., 2008. Robust Parameter Estimation in Gauged and Ungauged Basins, Ph.D.
653 dissertation No. 198, University of Stuttgart.

654

655 Sudheer, K. P., Gosain, A. K., & Ramasastri, K. S., 2002. A data-driven algorithm for
656 constructing artificial neural network rainfall–runoff models. *Hydrological Processes*, 16,
657 1325–1330.

658

659 Suryanarayana, C., Sudheer, C., Mahmood, V., & Panigrahi, B. K., 2014. An integrated
660 wavelet-support vector machine for groundwater level prediction in Visakhapatnam, India.
661 *Neurocomputing*, 145, 324-335.

662

663 Swain, R., & Sahoo, B., 2015. Variable parameter McCarthy–Muskingum flow transport
664 model for compound channels accounting for distributed non-uniform lateral flow. *Journal of*
665 *Hydrology*, 530, 698-715.

666

667 Tehrany, M. S., Pradhan, B., & Jebur, M. N., 2014. Flood susceptibility mapping using a
668 novel ensemble weights-of-evidence and support vector machine models in GIS. *Journal of*
669 *Hydrology*, 512, 332-343.

670

671 Tehrany, M. S., Pradhan, B., Mansor, S., & Ahmad, N., 2015. Flood susceptibility
672 assessment using GIS-based support vector machine model with different kernel
673 types. *Catena*, 125, 91-101.

674

675 Tiwari, M.K., & Chatterjee, C., 2010. Development of an accurate and reliable hourly flood
676 forecasting model using wavelet–bootstrap–ANN (WBANN) hybrid approach. *Journal of*
677 *Hydrology* 1 (394), 458–470.

678

679 Todini, E., 2007. A mass conservative and water storage consistent variable parameter
680 Muskingum-Cunge approach. *Hydrology and Earth System Sciences Discussions*, 4(3), 1549-
681 1592.

682

683 Uhlenbrook, S., Seibert, J., Leibundgut, C., & Rodhe, A., 1999. Prediction uncertainty of
684 conceptual rainfall-runoff models caused by problems to identify model parameters and
685 structure. *Hydrological Sciences Journal* 44, 779–798.

686

687 Vapnik, V. N., 1995. *The Nature of Statistical Learning Theory*. Springer-Verlag, New York,
688 USA. 314 p.

689

690 Yadav, B., Mathur, S., & Yadav, B. K. 2018. Data-based modelling approach for variable
691 density flow and solute transport simulation in a coastal aquifer. *Hydrological Sciences*
692 *Journal*, 1-17.

693

694 Yadav, B., & Eliza, K., 2017. A hybrid wavelet-support vector machine model for prediction
695 of Lake water level fluctuations using hydro-meteorological data. *Measurement*, 103, 294-
696 301.

697

698 Yadav, B., Ch, S., Mathur, S., & Adamowski, J., 2016a. Estimation of in-situ bioremediation
699 system cost using a hybrid Extreme Learning Machine (ELM)-particle swarm optimization
700 approach. *Journal of Hydrology*, 543, 373-385.

701

702 Yadav, B., Ch, S., Mathur, S., & Adamowski, J. 2016b. Discharge forecasting using an online
703 sequential extreme learning machine (OS-ELM) model: a case study in Neckar River,
704 Germany. *Measurement*, 92, 433-445.

705

706 Yadav, B., Perumal, M., & Bardossy, A., 2015. Variable parameter McCarthy–Muskingum
707 routing method considering lateral flow. *Journal of Hydrology*, 523, 489-499.

708

709 Yao, X., Tham, L., & Dai, F., 2008. Landslide susceptibility mapping based on support
710 vector machine: a case study on natural slopes of Hong Kong, China. *Geomorphology* 101,
711 572–582.

712

713 Yang, J., L., Y., Tian, Y., Duan, L., & Gao, W. Group-sensitive multiple kernel learning for
714 object categorization. In ICCV, 2009.

715

716 Yu X., Liong S., & Babovic V., 2004. EC-SVM approach for real-time hydrologic
717 forecasting. *Journal of Hydroinformatics*, 6 (3) 209–223.

718